

Library of dispersion-corrected atom-centered potentials for generalized gradient approximation functionals: Elements H, C, N, O, He, Ne, Ar, and Kr

I-Chun Lin, Maurício D. Coutinho-Neto,* Camille Felsenheimer, O. Anatole von Lilienfeld,†
Ivano Tavernelli, and Ursula Rothlisberger‡

Laboratoire de Chimie et Biochimie Computationnelle, Ecole Polytechnique Fédérale de Lausanne, Lausanne, CH-1015, Switzerland

(Received 2 February 2007; revised manuscript received 28 March 2007; published 31 May 2007)

Parameters for analytical dispersion-corrected atom-centered potentials (DCACPs) are presented to improve the description of London dispersion forces within the generalized gradient approximation functionals BLYP, BP, and PBE. A library of DCACPs for hydrogen, carbon, nitrogen, oxygen, helium, neon, argon, and krypton was obtained by calibrating against high-level CCSD(T) or configuration interaction references. The performance and transferability of DCACPs were tested on weakly bound complexes and provide excellent results throughout all investigated systems.

DOI: [10.1103/PhysRevB.75.205131](https://doi.org/10.1103/PhysRevB.75.205131)

PACS number(s): 31.15.Ew, 31.50.Bc, 31.70.-f

I. INTRODUCTION

London dispersion forces are of primordial importance in chemical and biological systems. Kohn-Sham density functional theory (KS-DFT),¹ with local density approximation (LDA) or present-day generalized gradient approximation (GGA) exchange correlation (xc) functionals, either provides sporadic results or fails completely to account for these forces.²⁻⁵ Consequently, considerable efforts have been made to remedy this shortcoming.⁵⁻¹¹

Dispersion-corrected atom-centered potentials (DCACPs) represent the effect of dispersion forces via additive atomic-orbital-dependent potentials whose two parameters are obtained by calibrating against references of chosen accuracy.¹² The first generation of DCACPs calibrated against MP2 references has already shown promising results.¹³⁻¹⁵

Herein, a procedure is described to obtain the DCACP parameters with a new penalty functional introduced to improve the long-range description of intermolecular interactions. A library of DCACPs, including parameters for hydrogen, carbon, nitrogen, oxygen, helium, neon, argon, and krypton, to be used in conjunction with BLYP,^{16,17} BP,^{16,18} and PBE¹⁹ functionals, is presented. DCACPs can be tuned to reach any desired accuracy given by the chosen reference. In this work, DCACPs were calibrated against high-level correlated *ab initio* CCSD(T) or CI references of (H₂)₂ in a parallel conformation,²⁰ benzene dimer (as sandwich),²¹ (N₂)₂ (parallel), (CO₂)₂ (cross shaped), and rare gas dimers.²² The calibration systems were chosen in order to fulfill the following criteria: (a) the system is small enough so that reference calculations are tractable, (b) the interaction energy is dominated by the balance between Pauli repulsion and dispersion forces, and (c) the electronic structures of the monomers in the complex are well described by the GGA employed. Testing was restricted to simple van der Waals (vdW) complexes where high-level reference data are available. Furthermore, the influence of DCACPs on intramolecular geometries and electronic structures was investigated by analyzing bond lengths, vibrational frequencies, electron densities, multipole moments, and polarizabilities. The compatibility of DCACPs with various atomic pseudopotential types was also addressed.

II. METHOD

In our approach, a penalty functional \mathcal{P} composed of two energy and one nuclear force dependent terms is introduced. Compared with the scheme in Ref. 12, an additional energy term evaluated at the (midpoint) distance where the interaction energy is half of the equilibrium energy is added to improve the long-range behavior of the resulting interaction energy curves. Note, however, that the asymptotic r^{-6} behavior is not explicitly imposed. The functional being minimized is given by

$$\min_{\{\sigma_i\}} \mathcal{P}(r) = \min_{\{\sigma_i\}} \left[|E^{\text{ref}}(r_{\text{min}}) - E(r_{\text{min}}, \{\sigma_i\})|^2 + |E^{\text{ref}}(r_{\text{mid}}) - E(r_{\text{mid}}, \{\sigma_i\})|^2 + \sum_I w_I |F_I(r_{\text{min}}, \{\sigma_i\})|^2 \right],$$

where r_{min} and r_{mid} are the intermolecular equilibrium and midpoint distances of the reference calculations. $E^{\text{ref}}(r)$ is the reference interaction energy at r , and w_I is a weighting factor, chosen so that contributions from the energy and the force terms (F_I) for atom I have the same order of magnitude. Only forces along the intermolecular interaction axis are considered.

This penalty functional is minimized by variationally tuning the $\{\sigma_i\}$ parameters that define the atom centered nonlocal potentials centered at $\{\mathbf{R}_i\}$:

$$v_I^{\text{DCACP}}(\mathbf{r}, \mathbf{r}') = \sum_{m=-l}^{+l} Y_{lm}(\hat{\mathbf{r}}) p_l(r) \sigma_l p_l(r') Y_{lm}^*(\hat{\mathbf{r}}'),$$

with the normalized projector $p_l(r) \propto r^l \exp[-r^2/(2\sigma_2^2)]$.

$r = |\mathbf{r} - \mathbf{R}_I|$ is the distance from the position of nucleus I , $\hat{\mathbf{r}}$ is the unit vector in the direction of $\mathbf{r} - \mathbf{R}_I$, and Y_{lm} denotes a spherical harmonic. This potential has the same analytical form as the nonlocal part of the atomic pseudopotentials developed by Goedecker *et al.*²³ We found that one projector is sufficient to obtain accurate results for the reference and test systems. Preliminary tests revealed that the method is insensitive to the choice of l for the expansion. Any angular momentum component not occupied in the atomic pseudopotentials can, in principle, be used, and we chose to standardize

TABLE I. DCACP parameters for H, C, N, and O in atomic units.

	BLYP		BP		PBE	
	$\sigma_1 [10^{-4}]$	σ_2	$\sigma_1 [10^{-4}]$	σ_2	$\sigma_1 [10^{-4}]$	σ_2
H	-4.06	2.71	-5.55	2.66	0.50	2.47
C	-5.49	3.11	-3.71	3.50	-5.79	2.84
N	-6.05	2.91	-8.06	2.82	-1.77	2.83
O	-7.92	2.57	-10.65	2.64	-6.47	1.73

on the rarely used component $l=3$. By tuning the amplitude (σ_1) and the width (σ_2) of DCACPs, \mathcal{P} is minimized in such a way that the reference equilibrium interaction energy and distance as well as the midpoint interaction energy are optimally reproduced for the calibration system. For this minimization, we employed a simple but robust simplex-downhill algorithm.²⁴

Even though in this communication we chose to concentrate only on three popular GGA functionals—BLYP, BP, and PBE—the DCACP approach is general and can be applied to any functionals. The LDA is accurate for solids and is still widely used in condensed matter physics. However, GGAs show a more consistent performance across various disciplines, including chemistry and biology, and offer a better description on intramolecular properties over LDA.

All DFT calculations were carried out using the program CPMD.²⁵ Pseudopotentials of Goedecker *et al.* type were used throughout the calibrations; for the testing calculations, Troullier-Martins²⁶ and Vanderbilt²⁷ types were also employed as specified. For the calibrations, we used plane-wave cutoffs (referred to as cutoff from now on) of 100 Ry (C and Ar), 120 Ry (He), 125 Ry (N), 150 Ry (H, O, Ar, and Kr), 550 Ry (Ne, for PBE and BP), and 600 Ry (Ne, BLYP). The calibrations of H, He, Ar, and Kr were carried out in an isolated $10 \times 10 \times 20 \text{ \AA}^3$ cell using the Poisson solver as implemented in CPMD according to Ref. 28. The calibration of neon was carried out in an isolated cell of $10 \times 10 \times 15 \text{ \AA}^3$ (BLYP) and $10 \times 10 \times 18 \text{ \AA}^3$ (BP and PBE). N ($10 \times 10 \times 20 \text{ \AA}^3$ cell) and C and O ($15 \times 15 \times 20 \text{ \AA}^3$ cell) were calibrated with periodic boundary conditions (PBCs). Unless otherwise stated, calibration references were calculated at the CCSD(T)/aug-cc-pVTZ level of accuracy with the GAUSSIAN03 package.²⁹ The test calculations were set up as follows: 150 Ry cutoff, $10 \times 10 \times 20 \text{ \AA}^3$ (20 \AA on the intermolecular axis) cell with PBCs for Ar-N₂ complexes; 100 Ry cutoff, isolated $12 \times 12 \times 30 \text{ \AA}^3$ cell for formaldehyde dimer; 100 Ry cutoff, $15 \times 15 \times 15 \text{ \AA}^3$ cell with PBCs for H₂-benzene complex.

III. RESULTS AND DISCUSSIONS

A. Parameters

Tables I and II list the DCACP parameters for H, C, N, and O and the rare gas atoms He, Ar, Ne, and Kr to be used in combination with the GGA functionals BLYP, BP, and PBE. The radial term of DCACPs is plotted in the form of $-\sigma_1^{1/2} p_{l=3}(r)$ in Fig. 1.

TABLE II. DCACP parameters for rare gas atoms in atomic units.

	BLYP		BP		PBE	
	$\sigma_1 [10^{-4}]$	σ_2	$\sigma_1 [10^{-4}]$	σ_2	$\sigma_1 [10^{-4}]$	σ_2
He	-3.92	2.40	-9.91	2.16	3.31	1.98
Ne	-6.41	2.48	-12.92	2.42	3.00	2.07
Ar	-12.96	2.77	-16.42	2.79	-7.44	2.15
Kr	-12.95	3.18	-14.68	3.22	-3.48	3.20

A positive σ_1 indicates that the original xc functional produces overbinding curves whereas a negative σ_1 shows that the uncorrected interaction energy curve is underbinding. While the BLYP and BP intermolecular interaction curves are always repulsive for the calibration systems, PBE shows partial binding in some cases. As a result, DCACPs for BLYP and BP have consistently negative σ_1 while no obvious trend can be observed for DCACPs complementing PBE. For the latter, σ_1 varies according to the performance of uncorrected PBE.

B. Calibrations

Figure 2 shows the interaction energy curves of (H₂)₂ calculated using DCACPs calibrated with and without the midpoint term in the penalty functional. The inclusion of the midpoint term significantly improves the midrange to long-range behavior; however, in order to satisfy this additional penalty term, compromises are made: r_{\min}^{DCACP} for DCACP-PBE is shifted outwards by 0.06 Å with respect to r_{\min}^{CI} and the interaction energy is more attractive by 0.002 kcal/mol. DCACP-BLYP behaves slightly worse: r_{\min}^{DCACP} is shifted out by 0.12 Å compared to r_{\min}^{CI} and the complex is overstabilized by 0.007 kcal/mol. Bearing in mind that the interaction energy curve is shallow around the minimum, this shift is negligible for simulations performed at finite temperatures. Better fitting results for the equilibrium energies and distances were obtained for all other calibration systems using the midpoint penalty functional.

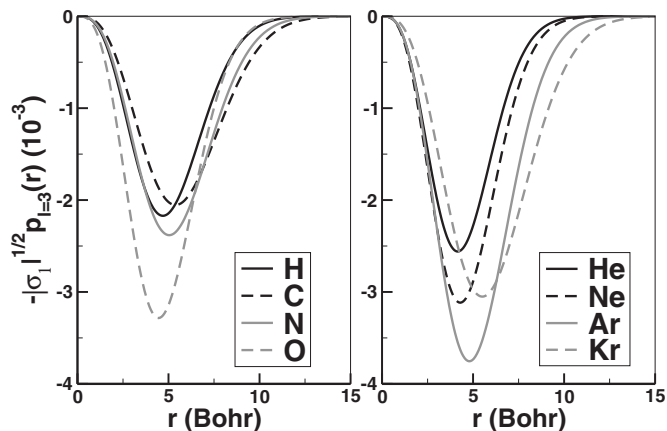


FIG. 1. The radial term of DCACPs complementing the BLYP functional plotted in the form of $-\sigma_1^{1/2} p_{l=3}(r)$.

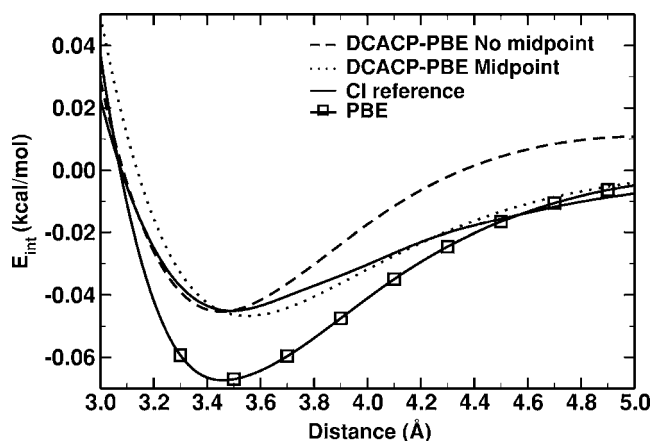


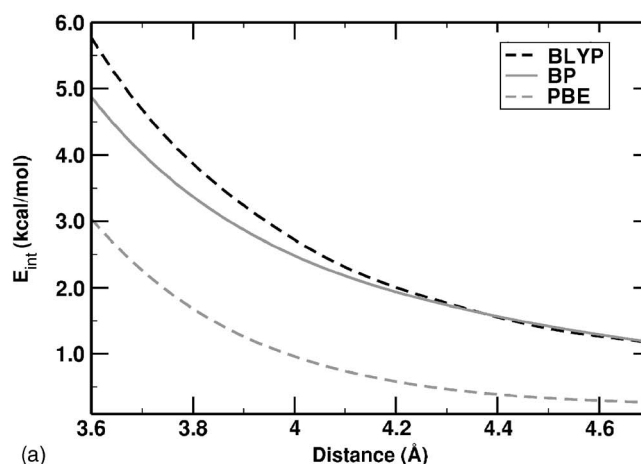
FIG. 2. Interaction energy curve of parallel H_2 dimers as a function of intermolecular distance showing the effect of including the midpoint term in the penalty functional.

Figure 3 shows the interaction energy curves of the sandwich benzene dimer as an example of the DCACP's performance on a calibration system. The overall shape of the interaction energy curves calculated at the same level of accuracy as the reference points [CCSD(T)] and the ones evaluated with the DCACP-augmented xc functionals (DCACP-GGA) agree very well, considering that there are only three penalty terms (two energy- and one nuclear-force-dependent terms) and only two adjustable parameters per element. For the rare gas dimers, r_{\min} and E_{\min} are also in very good agreement with the reference values, in great contrast to the spurious attractive or repulsive behavior of the unaugmented xc functionals.

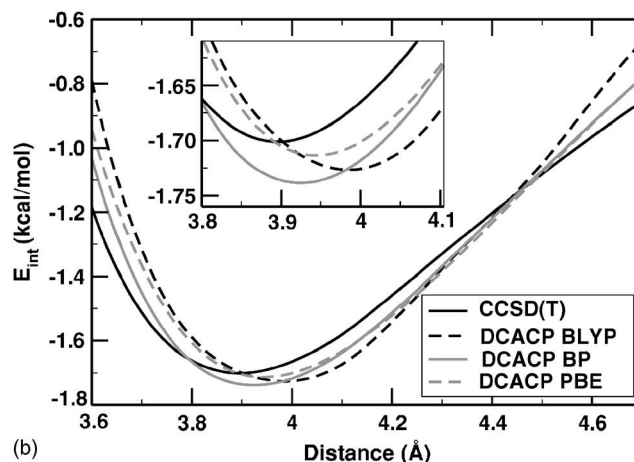
C. Effects on electronic structure

The fact that DCACPs occupy a polarization channel and are much weaker as well as longer ranged than the atomic pseudopotentials should ensure that there is no interference between the two. To verify this, we checked the effect of DCACPs on molecular geometries. Specifically, the bond lengths of the isolated monomers of the calibration systems, including single, double, and triple bonds, were computed. The values obtained with DCACP-GGA deviate negligibly from those of the corresponding uncorrected functionals (one thousandth of an Å). Furthermore, dynamical properties were tested via vibrational frequency analysis on geometry-optimized (ionic gradient tolerance of 10^{-5} a.u.) molecular hydrogen, water, and carbon dioxide and showed small deviations of $\leq 5 \text{ cm}^{-1}$.

Unlike the DFT-D scheme⁷ in which an explicit force field-like the r^{-6} dependence is included, DCACPs are effective potentials whose contributions to the total energy depend explicitly on the electronic wave function. As a consequence, DCACPs adapt to the chemical environment where the atom is—i.e., exhibit strongly improved transferability properties. On the other hand, it is not desirable to have DCACPs strongly affecting the already reasonably well-described electronic properties. In this regard, the very small amplitude of DCACPs (10^{-4} – 10^{-5} smaller than the



(a)



(b)

FIG. 3. Interaction energy curves of the sandwich benzene dimer as a function of intermolecular distance with (a) pure and (b) DCACP-augmented GGA functionals.

atomic pseudopotential) induces a negligible effect on characteristic properties that depend on the electronic structure: properties such as polarizabilities and multipole moments (tested on formaldehyde, Ar, CO_2 , N_2 , and benzene) remain basically unchanged. Figure 4 illustrates that the effect of DCACPs on the electronic structure of a vdW complex is small (the largest electron density difference is 10^{-4} smaller than the complex's maximum electron density) but relevant: there is an increase of electron density in the intermolecular space at the expense of the density on the molecular plane.

D. Transferability

The assessment of the newly generated DCACPs was limited to a simple set of weakly bound complexes. Even though the size of the testing set is relatively small and restricted to the gas phase only, the transferability of the parameters is expected to be at least on par with the ones calibrated against MP2 references where encouraging results were obtained for rare gases, graphene, and hydrocarbon complexes.^{12,13} Furthermore, recent studies employing DCACPs with BLYP functional successfully described condensed phase phenomena such as the binding energy of graphene sheets, the cohe-

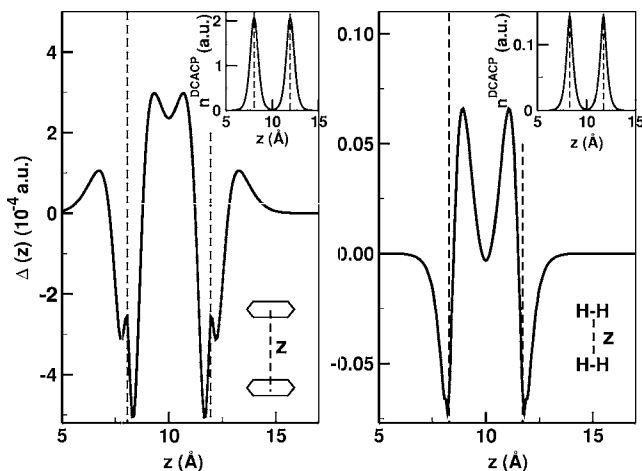






FIG. 4. Graphs showing $\Delta(z) = \int dx dy [n^{\text{DCACP}}(\mathbf{r}) - n^{\text{BLYP}}(\mathbf{r})]$ [atomic units (a.u.)] against the intermolecular axis z (Å) for the benzene dimer (left) and the H_2 dimer (right). The dotted lines show the position of the moieties. The inset shows the DCACP-BLYP electron density for the respective system.

sive energy of benzene crystal³⁰ and properties of liquid water.³¹

Here, the interaction energy of H_2 -benzene (bound by dispersion forces), Ar-N_2 complexes in two different configurations (bound by dispersion forces), and formaldehyde (H_2CO) dimer (bound by dipole-dipole interaction and dispersion forces) were evaluated with fixed monomer geometry. The results are tabulated in Table III. GGA functionals fare badly in describing these complexes where the dominate forces are weak interactions: the minimum interaction energy

TABLE III. Equilibrium distance (Å) and interaction energy (kcal/mol) of weakly bound complexes. Results from DCACP-GGA are marked with an asterisk. For repulsive interaction curves, the quoted interaction energy is calculated at the equilibrium distance of the corresponding DCACP complex.

								
	E_{min}	r_{min}	E_{min}	r_{min}	E_{min}	r_{min}	E_{min}	r_{min}
BLYP	0.47	2.90	-0.91	3.8	0.23	4.40	0.34	3.80
BLYP*	-1.06	2.90	-2.35	3.3	-0.15	4.40	-0.25	3.80
BP	0.56	2.75	-0.71	3.6	0.35	4.41	0.52	3.76
BP*	-1.24	2.75	-2.39	3.2	-0.11	4.41	-0.26	3.76
PBE	-0.48	3.05	-1.55	3.4	-0.12	4.45	-0.12	3.98
PBE*	-0.96	2.85	-2.06	3.3	-0.20	4.31	-0.24	3.80
CCSD(T) ^a	-0.95	2.75	-2.18	3.3	-0.23	4.26	-0.30	3.70

^aReference: Ar-N_2 (Ref. 32), $\text{H}_2\text{-C}_6\text{H}_6$ (Ref. 33), H_2CO dimer calculated in this work with aug-cc-pVDZ basis set

E_{min} is overly underestimated [mean absolute error (MAE) 0.80 kcal/mol] and the equilibrium distance r_{min} , if predicted at all, is shifted out, sometimes by as much as 0.6 Å. BLYP (MAE 0.95 kcal/mol) and BP (MAE 1.10 kcal/mol) fail to predict minima in all cases apart from the dipole-dipole interaction-dominated formaldehyde dimer; PBE shows qualitative binding, albeit at the wrong r_{min} (MAE: 0.35 kcal/mol, 0.22 Å).

The inclusion of DCACPs greatly improves the performance: overall MAEs are reduced down to 0.08 Å and 0.11 kcal/mol for r_{min} and E_{min} , respectively. r_{min} is predicted extremely well throughout the set, with deviations of less than 0.2 Å from the CCSD(T) values. DCACP-PBE (shown as PBE* in the table) with a MAE of 0.05 kcal/mol stands out as the best among the three functionals tested (MAE: 0.10 and 0.16 kcal/mol for DCACP-BLYP and DCACP-BP, respectively). As mentioned previously, the DCACP parameters depend heavily on the performance of the corresponding GGA functionals. DCACPs complementing PBE can be either attractive or repulsive depending on the element in question, making it possibly more system dependent and thus less transferable. On the other hand, DCACPs for BP and BLYP always provide an attractive correction to the underlying functional, in line with the idea of a dispersion-motivated correction. Thus, we believe that the latter combinations may be preferable over the better-behaving DCACP-PBE due to the more clean-cut interpretations they offer.

As a side note, the Ar-N_2 complex (the linear form labeled *L* in Table III) shows the largest deviation of all test cases. Since r_{min} for this complex lies at a relatively distant 4.3 Å, this might be attributed to the slight discrepancy between the midrange to long-range description of DCACP-GGA and the actual r^{-6} asymptotic behavior.

Besides being applicable to different density functionals, DCACPs presented herein are not restricted to be employed with the analytical format of Goedecker *et al.*²³ The constraint on the analytical format is only enforced during calibration. Numerical pseudopotentials such as Troullier-Martins²⁶ (TM) or Vanderbilt²⁷ (VDB) types can be (and were) used alongside. The DCACP-PBE N_2 dimer is used as an illustration for this “pseudopotential transferability” and shows that the improvement brought about by DCACPs is equally good in all three cases with the usual wavefunction cutoff employed for each pseudopotential type (e.g. 70 Ry for TM). As a side note, a numerical version of DCACPs can easily be included as an extra channel (*f* channel in this case) in TM pseudopotentials.

IV. CONCLUSIONS

We presented a library of DCACPs calibrated against CCSD(T) and full CI (H only) calculations that can be used in combination with the GGA functionals BLYP, BP, and PBE. The results indicate that the effects of London dispersion forces can be well described within DFT-GGA with the DCACP approach without introducing any significant intramolecular distortions on geometries and electronic

structures. Furthermore, DCACPs display a strong transferability to systems other than the calibration ones; i.e., once calibrated, DCACPs can be applied in various chemical environments without further tuning the parameters. In brief, the DCACP approach shows promising outcomes despite its empiricism, suggesting a more physical interpretation underlying this remarkable performance. More elaborate applications of DCACPs on chemical and biological systems are in progress.

A library of DCACPs in analytic and numerical formats,

interaction energy data and intramolecular properties discussed in this communication can be obtained from Ref. 34.

ACKNOWLEDGMENTS

I.C.L. and O.A.v.L. acknowledge the Swiss National Science Foundation for its financial support (Grant No. 200020-108063/1). M.D.C.N. acknowledges support from BIOM-ACH, Priority 3 (NMP-2002-3.4.1.1-3: Contract No. 505487-1). We thank A. P. Seitsonen for discussions. Calculations were done at the EPFL central computing facilities.

*Current address: Centro de Ciências Naturais e Humanas, Universidade Federal do ABC, Rua Santa Adélia, 166 Santo André. São Paulo, Brazil BR-09.210-170.

†Current address: Department of Chemistry, New York University, New York, NY 10003, USA.

‡Electronic address: ursula.roethlisberger@epfl.ch; URL: <http://lcbpc21.epfl.ch>

¹W. Kohn and L. J. Sham, *Phys. Rev.* **140**, A1133 (1965).

²S. Kristyán and P. Pulay, *Chem. Phys. Lett.* **229**, 175 (1994).

³J. M. Pérez-Jordá and A. D. Becke, *Chem. Phys. Lett.* **233**, 134 (1995).

⁴E. J. Meijer and M. Sprik, *J. Chem. Phys.* **105**, 8684 (1996).

⁵W. Kohn, Y. Meir, and D. E. Makarov, *Phys. Rev. Lett.* **80**, 4153 (1998).

⁶M. Dion, H. Rydberg, E. Schröder, D. C. Langreth, and B. I. Lundqvist, *Phys. Rev. Lett.* **92**, 246401 (2004).

⁷S. Grimme, *J. Comput. Chem.* **25**, 1463 (2004).

⁸J. F. Dobson, J. Wang, B. P. Dinte, K. McLennan, and H. M. Le, *Int. J. Quantum Chem.* **101**, 579 (2005).

⁹A. J. Misquitta, R. Podeszwa, B. Jeziorski, and K. Szalewicz, *J. Chem. Phys.* **123**, 214103 (2005).

¹⁰A. D. Becke and E. R. Johnson, *J. Chem. Phys.* **124**, 014104 (2006).

¹¹Y. Zhao and D. G. Truhlar, *J. Chem. Theory Comput.* **3**, 289 (2007).

¹²O. A. von Lilienfeld, I. Tavernelli, U. Rothlisberger, and D. Sebastiani, *Phys. Rev. Lett.* **93**, 153004 (2004).

¹³O. A. von Lilienfeld, I. Tavernelli, U. Rothlisberger, and D. Sebastiani, *Phys. Rev. B* **71**, 195119 (2005).

¹⁴A. Tkatchenko and O. A. von Lilienfeld, *Phys. Rev. B* **73**, 153406 (2006).

¹⁵O. A. von Lilienfeld and D. Andrienko, *J. Chem. Phys.* **124**,

054307 (2006).

¹⁶A. D. Becke, *Phys. Rev. A* **38**, 3098 (1988).

¹⁷C. Lee, W. Yang, and R. G. Parr, *Phys. Rev. B* **37**, 785 (1988).

¹⁸J. P. Perdew, *Phys. Rev. B* **33**, 8822 (1986).

¹⁹J. P. Perdew, K. Burke, and M. Ernzerhof, *Phys. Rev. Lett.* **77**, 3865 (1996).

²⁰H. Lavendy, J. M. Robbe, and J. P. Flament, *Chem. Phys. Lett.* **196**, 377 (1992).

²¹M. O. Sinnokrot and C. D. Sherrill, *J. Phys. Chem. A* **108**, 10200 (2004).

²²N. Kurita and H. Sekino, *Int. J. Quantum Chem.* **91**, 355 (2003).

²³S. Goedecker, M. Teter, and J. Hutter, *Phys. Rev. B* **54**, 1703 (1996).

²⁴W. H. Press, S. A. Teukolsky, W. T. Vetterling, and B. P. Flannery, *Numerical Recipes* (Cambridge University Press, Cambridge, England, 1986).

²⁵J. Hutter *et al.*, Computer code CPMD, version 3.8, IBM Corp. and MPI-FKF Stuttgart, 1990–2003, <http://www.cpmid.org>

²⁶N. Troullier and J. L. Martins, *Phys. Rev. B* **43**, 1993 (1991).

²⁷D. Vanderbilt, *Phys. Rev. B* **41**, 7892 (1990).

²⁸G. J. Martyna and M. E. Tuckerman, *J. Chem. Phys.* **110**, 2810 (1999).

²⁹M. J. Frisch *et al.*, Computer code GAUSSIAN 03, revision C.02, Gaussian, Inc., Wallingford, CT, 2004.

³⁰E. Tapavicza, I-C. Lin, O. A. von Lilienfeld, I. Tavernelli, M. D. Coutinho-Neto, and U. Rothlisberger (unpublished).

³¹I-C. Lin, A. P. Seitsonen, I. Tavernelli, M. D. Coutinho-Neto, and U. Rothlisberger (unpublished).

³²K. Patel, P. B. Butler, A. M. Ellis, and M. D. Wheeler, *J. Chem. Phys.* **119**, 909 (2003).

³³A. Ferre-Vilaplana, *J. Chem. Phys.* **122**, 104709 (2005).

³⁴<http://lcbpc21.epfl.ch/dcacp/dcacp.html>